Carbon Letters (2024) 34:723–730
https://doi.org/10.1007/s42823-023-00633-w

Online ISSN 2233-4998
Print ISSN 1976-4251

ORIGINAL ARTICLE

Carbon nanofiber electrodes derived from polyacrylonitrile/cucurbituril composite and their supercapacitor performance

Seung Ah Kim[1] · Hyeon Jin Park[1] · Seon Kyung Kim[1] · Kyeng Min Park[2] · Kyung-Hye Jung[1]

Received: 18 April 2023 / Revised: 25 August 2023 / Accepted: 21 October 2023 / Published online: 22 November 2023

Abstract

Porous carbon nanofiber (CNF) electrodes for supercapacitors were prepared by using polyacrylonitrile (PAN) and cucurbituril (CB), which is a macrocyclic compound comprising glycoluril units containing hollow cores. Mixture of PAN and CB in dimethyl sulfoxide was electrospun, and thermally treated to produce CNF electrodes. Their thermal stability, surface morphology, carbon microstructures, and surface porosity were investigated. Electrochemical properties were measured using three-electrode with synthesized CNFs without further treatment as a working electrode and 1 M Na_2SO_4 as an electrolyte. CNFs derived from PAN and CB exhibited a high specific capacitance of 183.5 F g^{-1} and an energy density of 25.4 Wh kg^{-1} at 0.5 A g^{-1} with stable cyclic stability during 1000 cycles, which is significantly higher than those for CNFs derived from PAN only. This demonstrated that the introduction of CB successfully improved the energy storage performance of CNF electrodes.

Keywords Supercapacitors · Carbon nanofibers · Cucurbituril · Polyacrylonitrile · Porous carbon electrodes

1 Introduction

Supercapacitors are one of the energy storage devices which have acquired considerable attention due to their fast charge, high power density, long life cycles, and temperature-independent performance [1, 2]. Recently, these advantages of supercapacitors allow them to be used as ancillary devices of electric and hybrid vehicles for acceleration and regenerative braking [3]. Supercapacitors include electrochemical double layer capacitors (EDLCs), pseudocapacitors, and hybrid capacitors [4]. Among them, EDCLs store the charge by electrostatic interactions on two symmetric electrodes, which are typically porous carbon materials such as activated carbon. Lack of the Faradaic redox reaction of carbon electrodes results in low capacitance and energy density of EDLCs, which limits their wide applications. Since energy storage performance of supercapacitors has a proportional relationship to contact area between electrode and electrolyte, enlarging surface porosity of electrode materials is considered as a good strategy to overcome this shortage.

Cucurbituril (CB) is a nonadecacyclic compound consisting of tetrazocane units fusing glycoluril moieties, which is synthesized from urea, glyoxal, and formaldehyde, and its shape resembles the shape of a pumpkin containing a hollow core [5, 6]. It was found that as the number of glycoluril units increases, the internal pore space of the ring becomes wider and the molecule becomes flexible [7]. Due to its exceptional binding ability and stable pore structures, CB has been investigated in a wide range of applications such as sensors, water treatment, and drug delivery and so on. It was reported that its porous structures are transferred after carbonization, making it an excellent precursor for supercapacitor electrodes [8].

✉ Kyeng Min Park
kpark@cu.ac.kr

✉ Kyung-Hye Jung
khjung@cu.ac.kr

Seung Ah Kim
tmddk554@naver.com

Hyeon Jin Park
dsa8487@naver.com

Seon Kyung Kim
seon3193@naver.com

[1] Department of Advanced Materials and Chemical Engineering, Daegu Catholic University, Gyeongsan-si, Gyeongbuk, Republic of Korea

[2] Department of Biochemistry, School of Medicine, Daegu Catholic University, Daegu, Republic of Korea

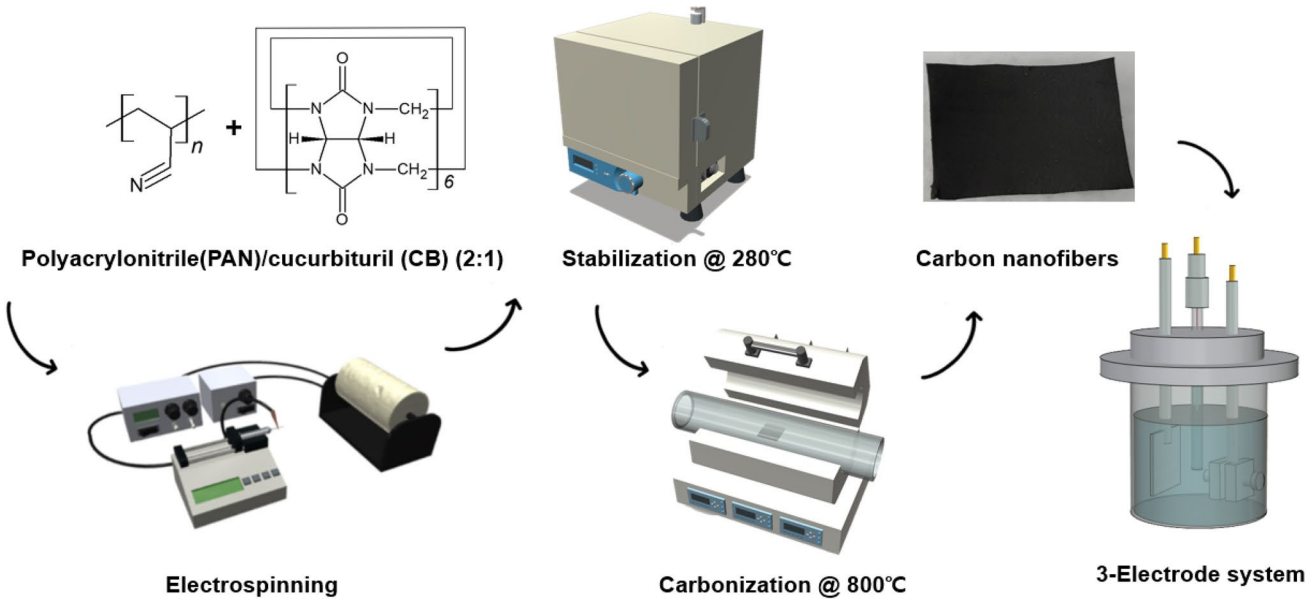

Scheme 1. Preparation of CNFs derived from PAN/CB

Carbon nanofibers (CNFs) are also good candidate for EDLC electrodes due to their high specific surface properties and good conductivity [9]. There are two synthesis methods: thermal treatment of electrospun nanofibers of precursor polymers, and chemical vapor deposition (CVD) using carbon precursors and metal catalyst [10, 11]. For the former method, the electrochemical performance of CNFs can be optimized by adjusting the chemical structures of precursor polymers, and the conditions for electrospinning and thermal treatments [12, 13]. Electrospinning is the most common way to fabricate nanofibers since the most of polymers and solvents can be applicable. It is also well-known that composite nanofibers can be readily produced by mixing additives in the polymer solutions, and then electrospinning them [14].

Most of the studies on CNFs for supercapacitor electrodes focus on the increase in surface area and porosity using sacrificial pore generating agents such as thermally degradable substance [15]. During the conversion of precursor polymers to carbon under high temperature, they are thermally decomposed creating pores in the CNF surface. It was also reported that precursor polymer blends can convert into porous carbon [16–18]. Investigating novel precursor composite or blends is critical to obtain highly porous CNFs with exceptional energy storage performance. Despite the outstanding pore structures of CB, limited research on CB in the field of energy storage has been conducted.

The present study is aimed at producing porous CNF electrode by thermal treatments of PAN/CB composite nanofibers to obtain high energy storage performance. CNFs can make them as free-standing electrodes without the use of binders while the addition of CB can improve the surface porosity of CNFs due to its stable pore structures. Surface morphology and carbon microstructures were investigated by scanning electron microscopy and Raman spectroscopy, respectively. Electrochemical properties were tested by assembling a three-electrode cell with pristine CNFs as a working electrode, and cyclic voltammetry (CV), galvanostatic charge–discharge, and cycling performance were investigated.

2 Experimental

Scheme 1 shows the preparation process of CNFs using PAN and CB. CB [6] consisting of 6 glycoluril subunits was chosen as a pore generator, and synthesized according to literature procedures [19]. Glycoluril was suspended in sulfuric acid, heated at 70 °C, and then formaldehyde dissolved in water was added. While the mixture was stirred at 70–75 °C for 24 h and at 95–100 °C for 12 h, crystalline CB [6] was precipitated. After pouring the reaction mixtures in water, acetone was added to produce precipitate. The mixture was filtered and washed with water and dried under vacuum. The chemical compositions of synthesized CB [6] were investigated using an attenuated total reflection (ATR)-Fourier transform infrared (FTIR) spectroscopy (VERTEX 80 V, Bruker, Ettlingen, Germany) with a germanium ATR crystal.

Seventeen wt% PAN/CB (2:1) dissolved in dimethyl sulfoxide (DMSO) was electrospun under an applied voltage range from 10 to 15 kV, and PAN only in DMSO was also prepared for comparison. Electrospun nanofibers were stabilized at

280 °C under air for 2 h and carbonized at 800 °C under nitrogen for 30 min to fabricate CNFs. From preliminary study, it concluded that electrochemical properties can be improved as the content of CB increases. CNFs derived from PAN/CB solutions with a ratio of 10:0, 9:1 and 2:1 were prepared and showed the energy densities of 13.4, 19.4 and 25.4 Wh kg^{-1}, respectively. It was also observed that the higher content of CB induces poor solubility and electrospinnability. Based on the electrochemical properties and spinnability, PAN/CB (2:1) was chosen. Carbonized PAN and PAN/CB were represented as cPAN and cPAN/CB, respectively.

Thermal stability was measured by thermogravimetric analysis (TGA) using a DTA-60, DSC-60, Shimadzu, Japan. The surface morphology of electrospun and carbonized PAN and PAN/CB nanofibers was observed using scanning electron microscopy (SEM) via an S-4800, Hitachi, Japan after sputter coating with osmium. Carbon microstructures of cPAN and cPAN/CB were studied by recording Raman spectroscopy using an XPLORA, Horiba, Japan. Surface area and porosity of CNFs were measured using nitrogen adsorption/desorption on an Autosorb iQ and a Quadrasorb SI (Quantachrome, USA). Specific surface area and pore size distribution were calculated using the Brunauer–Emmett–Teller (BET) equation and density functional theory (DFT) methods, respectively.

Electrochemical measurements were performed on an electrochemical workstation (WBCS3000S, Wonatech, KOREA) using a three-electrode cell consisting of Pt as the counter electrode, Ag/AgCl as the reference electrode, and cPAN and cPAN/CB nanofibers were directly used as the working electrode without further treatment. 1 M Na_2SO_4 was utilized as the electrolyte.

Cyclic voltammograms were recorded between 0 and 1.0 V (vs. Ag/AgCl) at various scan rates ranging from 10 to 100 mV s^{-1}. Galvanostatic charge/discharge (GCD) testing was conducted between 0 and 1.0 V (vs. Ag/AgCl) at different current densities of 0.5–6 A g^{-1}. The specific capacitance (C_{sp}, F g^{-1}) was measured using $C_{sp} = \frac{I\mathrm{d}t\mathrm{d}}{mV}$, where I_d is the discharge current (A), t_d the discharge time (s), m the mass of a working electrode (g), and V the voltage window (V). Energy density (E, Wh kg^{-1}) and power density (P, kW kg^{-1}) were calculated using $E = \frac{I\mathrm{d}t\mathrm{d}V}{2m}$ and $P = \frac{E}{t\mathrm{d}}$, respectively. Capacitance retention by GCD testing after 5000 cycles was measured to confirm the cycling stability. Electrochemical impedance spectra (EIS) were evaluated over the frequency range of 100 kHz and 0.1 Hz using a 0.01 V amplitude on a PEC-L01, Peccek, Japan.

3 Results and discussion

CB was synthesized and its chemical structures were studied by FTIR as shown in Fig. 1. It shows distinctive bands at 1717 cm^{-1} for the stretching vibration of C=O, at 1464 cm^{-1} for the banding vibration of C–H, and 3005 and 2930 cm^{-1} for the stretching vibration of C–H of methylene. Significant peak at 3440 cm^{-1} is assigned to O–H of the water.

PAN and CB were dissolved in DMSO and electrospun, followed by thermal treatments including stabilization under air and carbonization under inert gas. Surface morphology of electrospun and carbonized nanofibers was studied by observing SEM images as shown in Fig. 2. It is seen that both PAN and PAN/CB show continuous and uniform nanofibrous structure with average diameters of 660 nm and 730 nm, respectively. After stabilization at 280 °C and carbonization at 800 °C, they still have nanofibrous structure with reduced diameters of 470 nm for cPAN and 570 nm for cPAN/CB.

The thermal stability of synthesized CB, and electrospun PAN and PAN/CB-6 nanofibers was observed using TGA measurements with a heating rate of 10 °C min^{-1} from room temperature to 800 °C, as shown in Fig. 3. It seems the pyrolysis of PAN starts around 300 °C, and the oxidative stabilization temperature was generally based on it [20]. During stabilization, linear PAN chains are transformed into oriented cyclized ladder structures caused by thermal crosslinking, and thus the stabilization step determines the carbon yield and the graphitic structures resultant CNFs [21]. For CB, the weight loss around 250 °C may occur due to the loss of hydrated and coordinated water molecules [7, 22]. PAN/CB shows significant weight loss around 250 °C resulting from the decomposition of CB, which is also observed in a TGA curve of CB only. It is also seen that 50% of PAN/CB-6 remains at 800 °C, and the intermolecular interaction between nitrile groups in PAN and carbamide groups in CB may result in high thermal stability of PAN/CB.

The Microstructure of CNFs derived from PAN and PAN/CB was studied by measuring Raman spectroscopy,

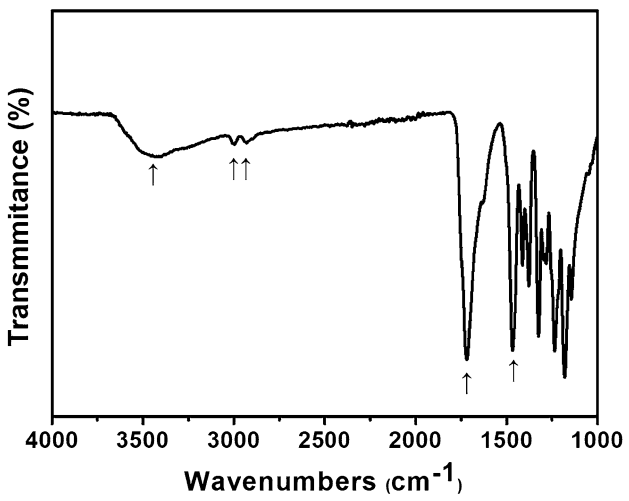

Fig. 1 FTIR spectrum of synthesized CB

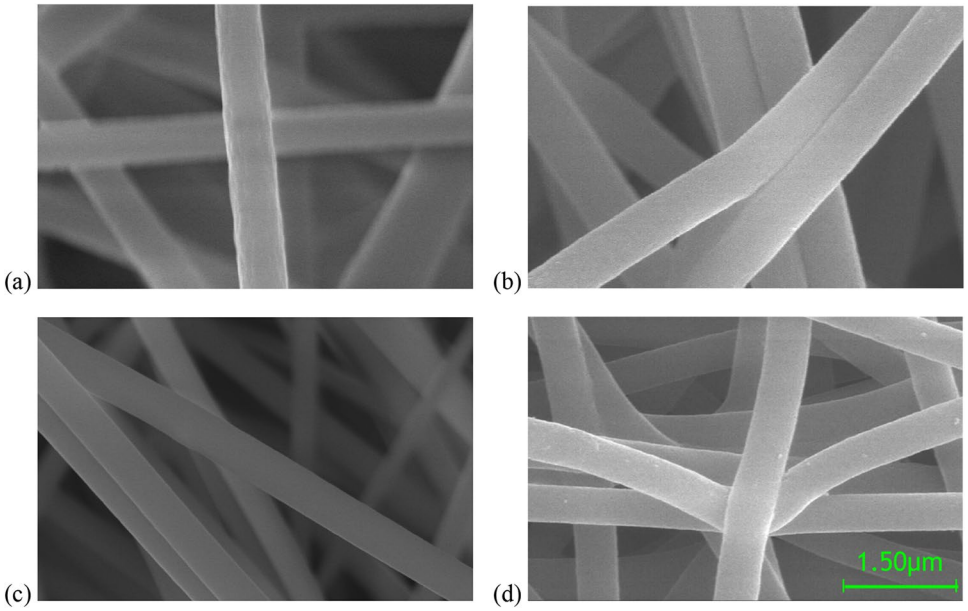

Fig. 2 Surface morphology of **a** as-spun PAN, **b** as-spun PAN/CB, **c** cPAN, and **d** cPAN/CB nanofibers

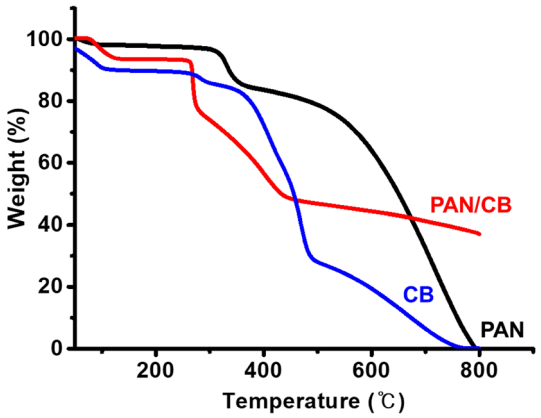

Fig. 3 Thermogravimetric analysis of **a** PAN, **b** CB and **c** PAN/CB

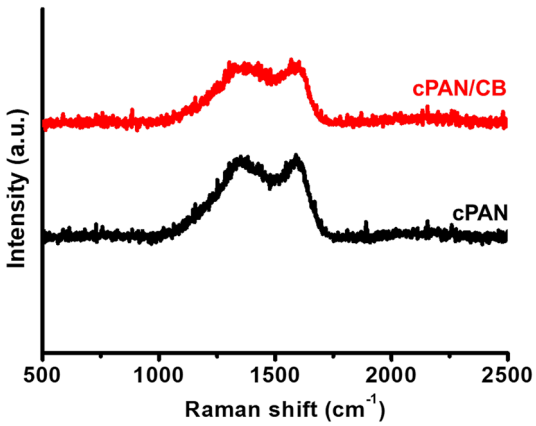

Fig. 4 Raman spectra of cPAN, and cPAN/CB

as shown in Fig. 4. Both cPAN and cPAN/CB indicated two significant peaks near 1585 and 1350 cm^{-1}, correlating with E_{2g2} graphitic crystallites (G-band) and disordered structure of carbon (D-band), respectively. This indicates the successful conversion of nanofibers into carbon via thermal treatments. The ratio of peak intensities (I_D/I_G), calculated using area under each curve, are 3.36 for cPAN and 3.56 for cPAN/CB, indicating predominantly disordered carbon derived from polymer precursors. Carbon materials derived from polymer precursors generally showed the high content of amorphous carbon. It was reported that the ratio of peak intensities is 2.9 for CNFs from PAN and 3.3 for CNFs from polybenzimidazole [20, 23, 24]. It was also known that carbonized CB is mainly composed of amorphous carbon phase [8].

Specific surface area and porosity were measured by nitrogen adsorption/desorption, as shown in Fig. 5, and specific surface area and pore volumes were calculated, as shown in Table 1. It is clearly seen that cPAN/CB exhibits higher surface area and pore volume than cPAN. It is also noticeable that cPAN/CB has significant increased meso-pore (with diameters in the range of 2–50 nm) volume of 0.140 cm^3g^{-1}, which is 26.9% of total pores. This means that the decomposition and carbonization of CB induce the creation of meso-pores on the CNF surface, and large pores of carbon electrodes can facilitate the access of electrolyte ions and improve the interfacial contact of ions between electrode/electrolyte [25].

Electrochemical properties of CNFs were measured in a three-electrode system with 1 M Na_2SO_4, and CNFs were used as a working electrode without adding any binders. Figure 6 exhibits cyclic voltammograms (CVs) of CNF electrodes, and both cPAN and cPAN/CB show typical CVs for

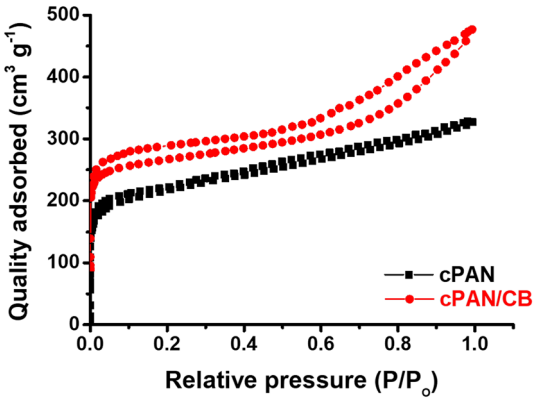

Fig. 5 Nitrogen adsorption/desorption isotherms of CNFs

Table 1 Structural parameters of cPAN and cPAN/CB

	SSA[a] (m^2g^{-1})	TPV[b] (cm^3g^{-1})	V_{micro} (cm^3g^{-1})	V_{meso} (cm^3g^{-1})
cPAN	604	0.334	0.327	0.007
cPAN/CB-6	812	0.521	0.381	0.140

V_{micro} micro-pore (<2 nm) volume, V_{meso} meso-pore (2–50 nm) volume

[a]SSA: specific surface area

[b]TPV: total pore volume

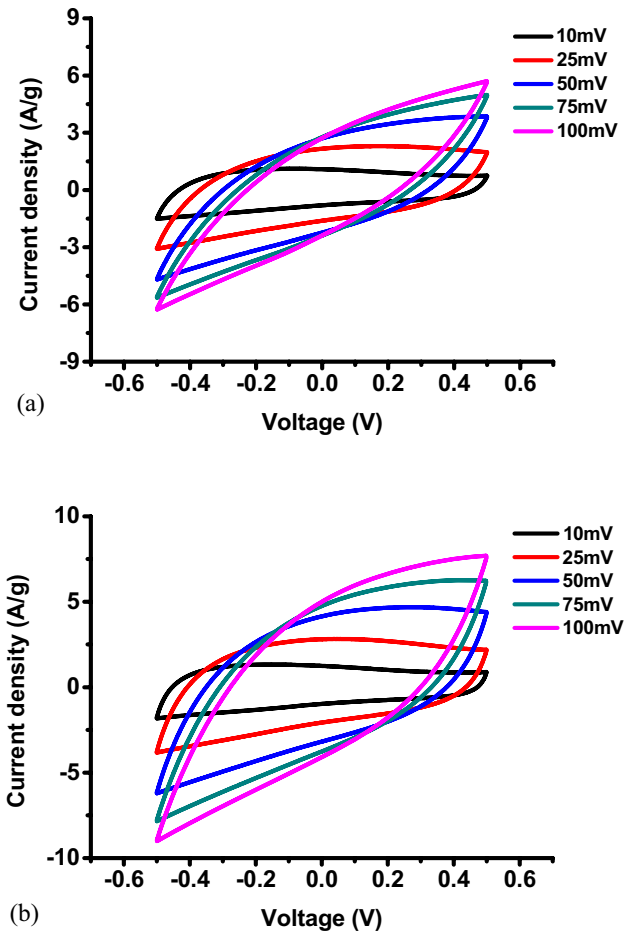

Fig. 6 Cyclic voltammograms of **a** cPAN, and **b** cPAN/CB electrodes

carbon electrode in EDLCs. It is obviously seen that cPAN/CB has higher current densities than cPAN over the whole voltage range (Fig. 7).

Galvanostatic charge–discharge testing was performed in the current density range from 0.5 to 6 A/g, the energy storage performance such as specific capacitance, and energy and power densities were calculated from the discharge curves from 1 to 0 V. Specific capacitances of cPAN and cPAN/CB are 96.5 and 183.5 F g^{-1} at 0.5 A/g, respectively. It is also seen that energy densities of cPAN and cPAN/CB are 13.4 and 25.4 Wh kg^{-1} at 0.5 A g^{-1}, respectively, while power densities show the identical value of 1.8 kW kg^{-1} at 6 A g^{-1}. Higher surface area and porosity caused by the existence of CB may result in significant higher energy storage performance.

For CNF electrodes synthesized via electrospinning, most of studies focus on enlarging surface porosity by adding pore generating materials. Polymers with poor thermal stability can be good candidates since they are decomposed during thermal treatment creating pores on the CNF surface. Poly-L-lactic acid (PLLA), poly (ethylene glycol) (PEG), and poly (methyl methacrylate) (PMMA) have been reported as pore generating materials, and CNFs from PAN showed high energy storage performance due to the enlarged surface area and porosity [26–28]. CB was chosen as pore generating materials since its stable cavity structures can generate pores on the CNF surface via thermal treatment. It is known that the cavity size of CB can be variable by controlling the number of glycoluril subunits [29, 30]. It was found that the width of cavities is ranged from 4.4 to 8.8 Å from CB [5] and CB [8], which can produce different size of pores when they are carbonized. It is known that an electrolyte is one of the critical parts to determine the energy storage performance by controlling the voltage window. Ionic liquid electrolytes show wide voltage window compared to aqueous ones (up to 1 V) [31, 32]. However, the bulkiness of their ions limits the access to the electrode surfaces, and it becomes more important enlarging surface area and porosity of electrode when ionic liquids are used as an electrolyte. It seems worthy to study the size of pores generated by various CBs and to match with size of ionic liquid ions, which can result in the optimization of energy storage performance.

It has been reported that high crystallinity of PAN is unfavorable to the cyclization during the stabilization step, in which the linear polymer chains are converted to an aromatic ladder structure [33]. Vinylimidazole and

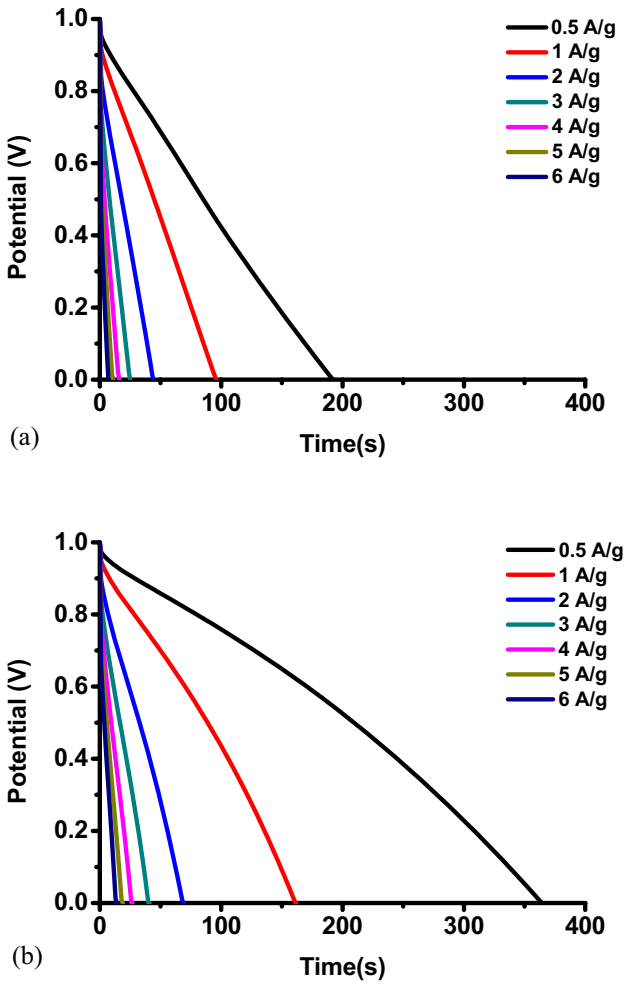

Fig. 7 Galvanostatic discharge curves of **a** cPAN, and **b** cPAN/CB electrodes

itaconic acid have been reported as effective comonomer candidates to disrupt the strong dipole–dipole interactions between nitrile groups in PAN and to reduce the crystallinity [34–37]. Small organic molecules such as CB can also play a role of a plasticizer to enhance the movement of PAN chains. It can be concluded that the introduction of CB is effective not only for increasing surface area and porosity, but for reducing crystallinity of PAN, resulting in superior energy storage performance the resultant CNFs.

EDLCs store their charge physically at the interface between electrodes and electrolyte without irreversible redox reactions, and thus exhibit long cycle life. Cycling stability of cPAN and cPAN/CB was evaluated by measuring specific capacitance at 1 A/g for every 250 cycles, as shown in Fig. 8. cPAN and cPAN/CB exhibit high capacitance retentions of 92.0% and 91.6% after 5000 cycles, respectively. A high degree of reversibility demonstrates the stable cyclic performance of the CNF electrodes.

Figure 9 shows EIS of cPAN and cPAN/CB electrodes. The size and shape of the semicircle at high frequency depend on the adsorption kinetics of ions at electrode pores, and on the resistances of materials and mass transfer while the slope of the plots in the low frequency region is related to the rate of the electrochemical double layer formation inside of the electrode pores [38]. cPAN/CB exhibits significantly lower impedance than cPAN, indicating the incorporation of CB effectively improves electric conductivity by enlarging the contact area and facilitating the charge transfer. Wu et al. reported that presence of pyrrolic-nitrogen and quaternary-nitrogen in carbonized CB, which are conductive to the electron conduction [8]. Thus, it is also expected that a higher content of nitrogen enables cPAN/CB to contain more conductive carbon matrix.

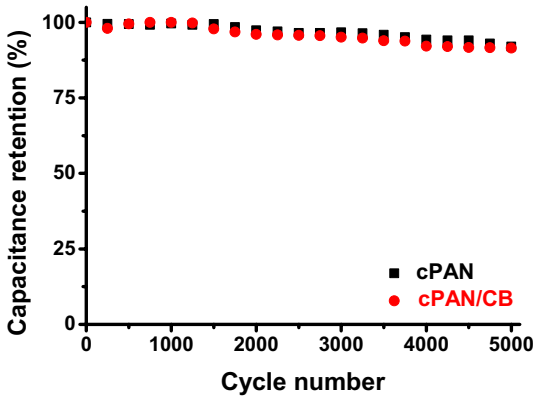

Fig. 8 Cyclic stability of cPAN, and cPAN/CB electrodes

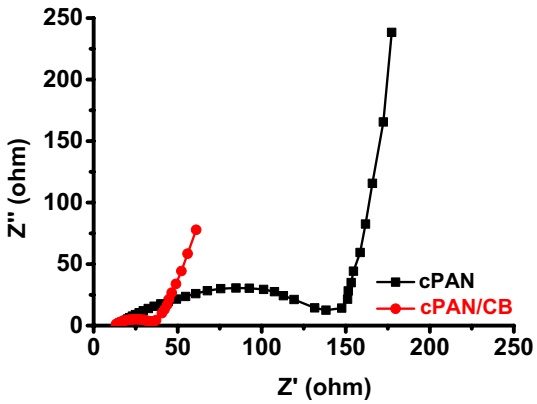

Fig. 9 EIS of cPAN, and cPAN/CB electrodes

4 Conclusion

CB was introduced as a pore generating material to produce porous CNF electrodes in supercapacitors. PAN/CB (2:1) solution in DMSO was prepared, electrospun, and thermally treated. Thermal stability of PAN/CB was confirmed by TGA, and the conversion of PAN/CB into CNFs was done by Raman spectroscopy. cPAN/CB showed significantly high specific surface area and meso-pore volumes compared to cPAN. Due to its superior surface properties, cPAN/CB exhibited exceptional energy storage performance such as a specific capacitance of 183.5 F/g and an energy density of 25.4 Wh/kg at 0.5 A/g with stable cyclic stability during 5000 cycles. It was also found that cPAN/CB has significantly lower impedance than cPAN, confirming PAN/CB composite is excellent precursor candidate as porous carbon for supercapacitor electrodes.

Acknowledgements This work was financially supported by Daegu Catholic University (20211122).

Data availability Data will be made available on request.

Declarations

Conflict of interest The authors declare that they have no known competing financial interests or personal relationships that could have appeared to influence the work reported in this paper.

References

1. Conway BE (1991) Transition from "supercapacitor" to "battery" behavior in electrochemical energy storage. J Electrochem Soc 138:1539
2. Conway BE (2013) Electrochemical supercapacitors: scientific fundamentals and technological applications. Springer Science & Business Media
3. Horn M, MacLeod J, Liu M, Webb J, Motta N (2019) Supercapacitors: a new source of power for electric cars? Econ Anal Policy 61:93
4. Li L, Wu Z, Yuan S, Zhang X-B (2014) Advances and challenges for flexible energy storage and conversion devices and systems. Enegy Environ Sci 7:2101
5. Mock WL, Shih NY (1986) Structure and selectivity in host-guest complexes of cucurbituril. J Org Chem 51:4440
6. Mock W, Shih N (1983) Host-guest binding capacity of cucurbituril. J Org Chem 48:3618
7. Santos GdC, Barros AL, de Oliveira CA, da Luz LL, da Silva FF, Demets GJ-F, Alves Júnior S (2017) New composites LnBDC@ AC and CB [6]@ AC: from design toward selective adsorption of methylene blue or methyl orange. PLoS ONE 12:e0170026
8. Zhu T, Song Z, Lin J, Wang Y, Sun S, Fan L, Lin J-Y, Wu J (2021) Cucurbit [8] uril-derived porous carbon as high-performance electrode material for ionic liquid-based supercapacitor. J Energy Storage 38:102527
9. Kim C (2005) Electrochemical characterization of electrospun activated carbon nanofibres as an electrode in supercapacitors. J Power Sources 142:382
10. Feng L, Xie N, Zhong J (2014) Carbon nanofibers and their composites: a review of synthesizing, properties and applications. Materials 7:3919
11. De B, Banerjee S, Verma KD, Pal T, Manna P, Kar KK (2020) Carbon nanofiber as electrode materials for supercapacitors. Handbook of nanocomposite supercapacitor materials II: Performance 179
12. Jung K-H, Panapitiya N, Ferraris JP (2018) Electrochemical energy storage performance of carbon nanofiber electrodes derived from 6FDA-durene. Nanotechnology 29:275701
13. Kim SJ, Son YJ, Jeon B, Han YS, Kim Y-J, Jung K-H (2020) Surface crosslinking of 6FDA-durene nanofibers for porous carbon nanofiber electrodes in electrochemical double layer capacitors. Nanotechnology 31:215404
14. Lei D, Li X-D, Ma M-J, Kim D-Y, Noh J-H, Kim B-S (2023) Salt-activated phenolic resin/PAN-derived core-sheath nanostructured carbon nanofiber composites for capacitive energy storage. Carbon Lett 1:699
15. Zhang L, Aboagye A, Kelkar A, Lai C, Fong H (2014) A review: carbon nanofibers from electrospun polyacrylonitrile and their applications. J Mater Sci 49:463
16. Abeykoon NC, Garcia V, Jayawickramage RA, Perera W, Cure J, Chabal YJ, Balkus KJ, Ferraris JP (2017) Novel binder-free electrode materials for supercapacitors utilizing high surface area carbon nanofibers derived from immiscible polymer blends of PBI/6FDA-DAM: DABA. RSC Adv 7:20947
17. Lee DG, Lee BC, Jung K-H (2021) Preparation of Porous Carbon Nanofiber Electrodes Derived from 6FDA-Durene/PVDF Blends and Their Electrochemical Properties. Polymers 13:720
18. Jung K-H, Ferraris JP (2012) Preparation and electrochemical properties of carbon nanofibers derived from polybenzimidazole/polyimide precursor blends. Carbon 50:5309
19. Kim J, Jung I-S, Kim S-Y, Lee E, Kang J-K, Sakamoto S, Yamaguchi K, Kim K (2000) New cucurbituril homologues: syntheses, isolation, characterization, and X-ray crystal structures of cucurbit [n] uril (n= 5, 7, and 8). J Am Chem Soc 122:540
20. Zhang W-x, Wang Y-z, Sun C-f (2007) Characterization on oxidative stabilization of polyacrylonitrile nanofibers prepared by electrospinning. J Polym Res 14:467
21. Zhou Z, Liu K, Lai C, Zhang L, Li J, Hou H, Reneker DH, Fong H (2010) Graphitic carbon nanofibers developed from bundles of aligned electrospun polyacrylonitrile nanofibers containing phosphoric acid. Polymer 51:2360
22. Germain P, Letoffe J, Merlin M, Buschmann H (1998) Thermal behaviour of hydrated and anhydrous Cucurbituril: A DSC, TG and calorimetric study in temperature range from 100 to 800 K. Thermochim Acta 315:87
23. Jung K-H, Ferraris JP (2016) Preparation of porous carbon nanofibers derived from PBI/PLLA for supercapacitor electrodes. Nanotechnology 27:425708
24. Wang Y, Serrano S, Santiago-Avilés JJ (2003) Raman characterization of carbon nanofibers prepared using electrospinning. Synth Met 138:423
25. Cui J, Yin J, Meng J, Liu Y, Liao M, Wu T, Dresselhaus M, Xie Y, Wu J, Lu C (2021) Supermolecule cucurbituril subnanoporous carbon supercapacitor (SCSCS). Nano Lett 21:2156
26. Pani TK, Sahoo BB, Sundaray B (2019) Carbon electrodes derived from polyacrylonitrile-polyethylene glycol blend for high-performance supercapcitor. Mater Res Express 6:125077
27. Dong W, Wang Z, Zhang Q, Ravi M, Yu M, Tan Y, Liu Y, Kong L, Kang L, Ran F (2019) Polymer/block copolymer blending system as the compatible precursor system for fabrication of mesoporous carbon nanofibers for supercapacitors. J Power Sources 419:137
28. Ji L, Zhang X (2009) Fabrication of porous carbon nanofibers and their application as anode materials for rechargeable lithium-ion batteries. Nanotechnology 20:155705

29. Atwood JL (2017) Comprehensive supramolecular chemistry II. Elsevier, Amsterdam
30. Barrow SJ, Kasera S, Rowland MJ, Del Barrio J, Scherman OA (2015) Cucurbituril-based molecular recognition. Chem Rev 115:12320
31. Largeot C, Portet C, Chmiola J, Taberna P-L, Gogotsi Y, Simon P (2008) Relation between the ion size and pore size for an electric double-layer capacitor. J Am Chem Soc 130:2730
32. Faisal MSS, Abedin F, Asmatulu R (2020) Activated carbons of pistachio and acorn shells for supercapacitor electrodes with TEABF 4/PC solutions as electrolytes. Carbon Lett 30:509
33. Yu M, Wang C, Bai Y, Wang Y, Xu Y (2006) Influence of precursor properties on the thermal stabilization of polyacrylonitrile fibers. Polym Bull 57:757
34. Faraji S, Yardim MF, Can DS, Sarac AS (2017) Characterization of polyacrylonitrile, poly (acrylonitrile-co-vinyl acetate), and poly (acrylonitrile-co-itaconic acid) based activated carbon nanofibers. J Appl Polym Sci 134:44381
35. Abeykoon NC, Mahmood SF, Yang DJ, Ferraris JP (2019) Electrospun poly (acrylonitrile-co-itaconic acid) as a porous carbon precursor for high performance supercapacitor: study of the porosity induced by in situ porogen activity of itaconic acid. Nanotechnology 30:435401
36. Jung K-H, Deng W, Smith DW Jr, Ferraris JP (2012) Carbon nanofiber electrodes for supercapacitors derived from new precursor polymer: Poly (acrylonitrile-co-vinylimidazole). Electrochem Commun 23:149
37. Jung K-H, Kim SJ, Son YJ, Ferraris JP (2019) Fabrication of carbon nanofiber electrodes using poly (acrylonitrile-co-vinylimidazole) and their energy storage performance. Carbon Lett 29:177
38. Eskusson J, Jänes A, Kikas A, Matisen L, Lust E (2011) Physical and electrochemical characteristics of supercapacitors based on carbide derived carbon electrodes in aqueous electrolytes. J Power Sources 196:4109